Column Axial Shortening Effects in Steel Frames

G. A. MacRae, K. Hyde, W. Walpole, P. Moss

University of Canterbury, Christchurch, New Zealand

C. Hyland

Steel Construction New Zealand, Manukau City, New Zealand

G. C. Clifton, N. Mago

Heavy Engineering Research Association, Manukau City, New Zealand

2006 NZSEE Conference

ABSTRACT: Steel members subject to constant axial compression and inelastic cyclic displacements exhibit axial shortening. This column axial shortening, which may occur during an earthquake, can cause undesirable effects in the building, especially if it occurs to different extents in different columns of a seismic-resisting system. This paper summarizes experiments, and finite-element analyses, used to model the axial shortening in a steel column. A method to minimize column axial shortening is then proposed and investigated with finite-element analyses. Future frame modelling to include axial shortening effects is described.

1 INTRODUCTION

Yielding is generally discouraged in columns of steel moment frames designed according to the Steel Structures Standard (SNZ, 1997) provisions and the detailed seismic design procedures of HERA Report R4-76 that utilize the strong-column/weak-beam concept. This is because:

i) columns tend to have lower monotonic deformation capacities than beams,
ii) column unidirectional hinging may occur during reversed cycling,
iii) column strength loss may be catastrophic,
iv) column yielding may lead to a soft story mechanism, and
v) column yielding may cause axial shortening and subsequent undesirable frame effects.

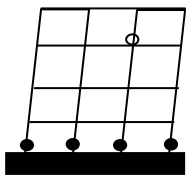

Figure 1. Expected Column Hinges in a Moment Frame

Nevertheless, because members in well-detailed steel framed structures are inherently ductile, column yielding is not totally restricted. Some column yielding may occur over the frame height due to dynamic earthquake effects as shown in Figure 1. Dynamic time history analyses of moment-resisting and eccentrically braced frames have shown that this yielding is not significant in most cases (e.g., MacRae, Walpole and Carr, 1990; Clifton, 2005). A significant amount of hinging may occur at the base of the frame in order to develop the full strong-column/weak-beam mechanism.

Relatively few tests have been carried out to evaluate the seismic behaviour of steel columns. It was after testing of columns with different axial loads under reversed cyclic lateral displacements at the University of Canterbury (MacRae, Walpole and Carr, 1990) that axial shortening was first reported. Columns tested were 250UC73 sections made from Grade 250 steel. They were subjected to 2 cycles to member displacement ductilities, μ, of 2, 4, 6, 8 etc., as shown in Figure 2, until the lateral force became less than 70% of the calculated strength. The change in length, Δ_a, for a column with a specific axial force ratio, N^*/N_y, ignoring the effect of buckling, was found to be approximately proportional to the cumulative inelastic rotation, $\Sigma\theta_H$, according to Equation 1. Here κ is an empirical factor dependent on N^*/N_y, and L_p is the plastic hinge length.

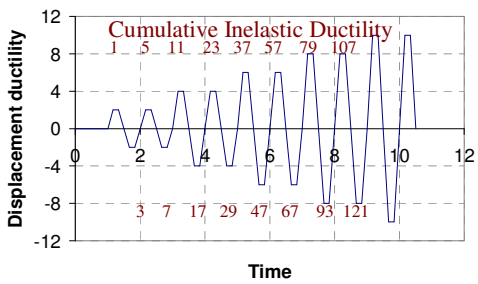

Figure 2. Typical Test Regime

$$\Delta_a = -\kappa L_p \Sigma\theta_H \quad (1)$$

$$\Sigma\theta_H = \Sigma\mu_H \, \delta_p / L_c \quad (2)$$

A decrease in the distance between the top and bottom of the column along the member axis indicates axial shortening. The cumulative inelastic rotation is related to the cumulative inelastic ductility, $\Sigma\mu_H$, by Equation 2, where δ_p is the displacement at the top of the cantilever column member associated with both the formation of the plastic moment at the column base and the initial stiffness of the column, and L_c is the column length. The cumulative inelastic ductility, $\Sigma\mu_H$, was computed as the inelastic component of an elastoplastic hysteretic curve from the test regime ductilities as shown in Figure 2.

As buckling became significant, the rate of axial shortening increased. The hysteretic loop for a column with an axial force of $0.40F_yA$, Column C4, and the axial displacement with cyclic loading is shown in Figure 3. More axial shortening occurred at the higher ductilities.

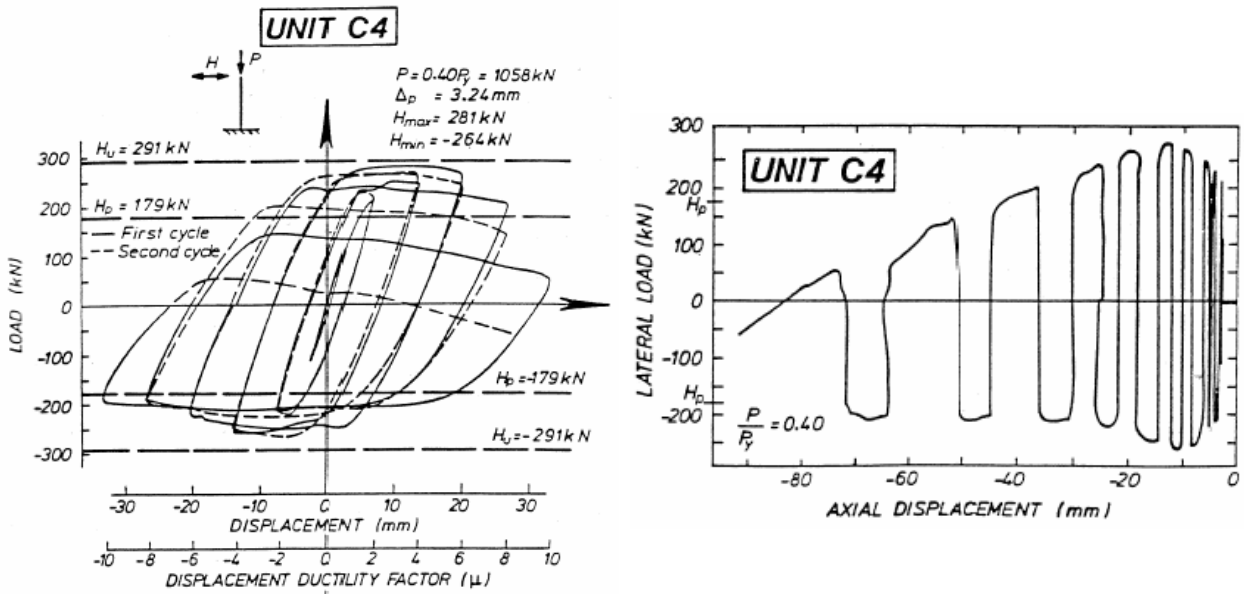

(a) Hysteretic Behaviour (H-Δ) (b) Axial Shortening, Δ_a

Figure 3. Behaviour of a Column with an Axial Force Ratio, N^*/N_y, of 0.40

For different levels of axial force, the relationship between the axial shortening, $-\Delta_a$, and the cumulative inelastic rotation, $\Sigma\theta_H$, is given in Figure 4. Higher axial forces are associated with greater shortening. The curves are initially linear and then the rate of axial shortening increases as a result of buckling. Equations are given for the linear part of these curves on the figure. L_p was assumed to equal the member depth, D. For high axial loads, the axial displacement was not dependent on the axial force ratio.

The reason for the behaviour in Figure 4 may be explained using Figure 5. Here, when the axial force ratio, N^*/N_y, is zero, there is (ideally) no axial shortening because there is no net strain at the centre of the section. When the section axial force ratio, N^*/N_y, is less than the ratio of the web area to the total area, A_w/A, the neutral axis will be in the web, and the axial force will effect the location of the neutral axis as well as the strain at the centre of the section, ε_c. For axial force ratios, N^*/N_y, greater than A_w/A, the position of the neutral axis and ε_c are not significantly affected by changes in N^*/N_y. In this case, the axial shortening, Δ_a, may be computed as the strain at the centre of the section, ε_c, multiplied by the total plastic hinge length, L_p. Here, ε_c is equal to the curvature of the section, $-\phi$, multiplied by the distance from the neutral axis to the centre of the section, which is approximately one half of the section depth, $D/2$. For inelastic strains that affect the axial shortening, the curvature may be

approximated as the inelastic rotation, θ_H, divided by the plastic hinge length, L_p. Following this reasoning the axial shortening is independent of the plastic hinge length, L_p, as shown in Equation 3. Equation 3 is consistent with the experimentally obtained data for columns with high axial forces and no buckling in Figure 4.

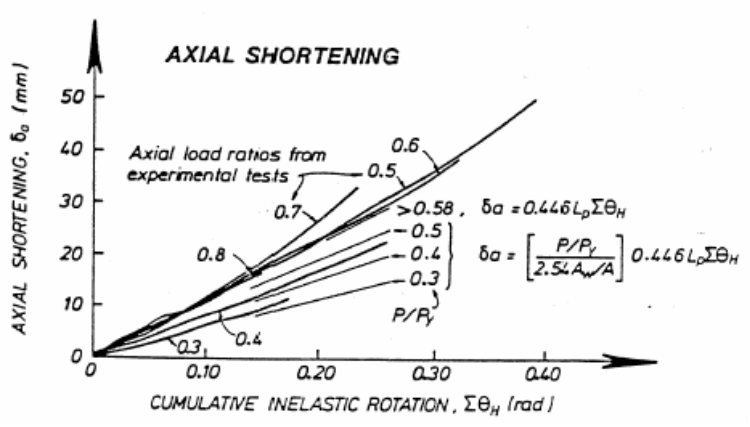

Figure 4. $-\Delta_{a\ and}\ \theta_H$ Relationship for all Columns

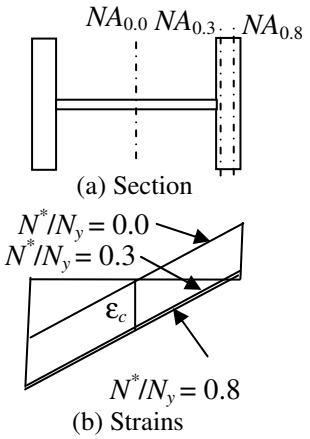

Figure 5. Position of NA for Different Column Axial Force Ratios, N^*/N_y

$$\Delta_a \quad = \varepsilon_c L_p \quad = -\phi.D/2.L_p \quad = -\theta_H/L_p.D/2.L_p \quad = -\theta_H.D/2 \tag{3}$$

The strains in Figure 5 are shown for monotonic loading. For reversed cyclic loading the neutral axis moves from one side of the section to the other, and back again, each cycle causing strains related to ε_c at the centre of the section.

Equation 4 was derived for axial shortening using the concepts described above. While Equation 4 is reasonable for axial force ratios greater than about 0.58, it overestimates the experimental shortening for low axial forces. For this reason, it is different from the equations shown in Figure 4 which are fitted to the actual experimental results.

$$\Delta_a \begin{cases} = -0.5\ (N^*/N_y)/(A_w/A)\ .\ D\ \Sigma\mu_H\ \ \delta_p/L_c & \text{when } N^*/N_y \le A_w/A \\ = -0.5\ D\ \Sigma\mu_H\ \ \delta_p/L_c & \text{when } N^*/N_y > A_w/A \end{cases} \tag{4}$$

If the amount of axial shortening were very small, it would not have an impact on building behaviour. However, the observed axial shortening at failure was as large as 78mm. This is equivalent to an axial strain of 7% over a cantilever height of 1.10m. This could relate to a displacement of 200mm or more in the bottom story of a real frame. MacRae et al. (1990) showed that the axial shortening was the main parameter affecting the deformation capacity of these compact columns. It can also result in relative vertical displacements of columns as shown in Figure 6. Here, it is assumed that only the centre column yields and shortens in the storey shown. This type of deformation may be difficult to repair.

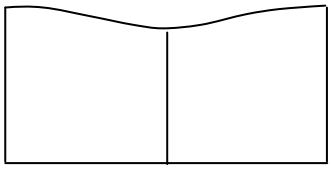

Figure 6. Column Axial Shortening in One Storey of a Frame

2 FINITE ELEMENT STUDY

The computer program ABAQUS (2004) was used to perform the finite element analysis of the column. It was modelled using a three dimensional 8-node linear brick element, type C3D8R, with reduced integration hourglass control. Symmetrical partitioning was used to minimize element distortion and the mesh was generated using a global seed size of 0.1, curvature control, and a deviation factor of 0.1. The final mesh is shown in Figure 7. The steel was assumed to have an elastic modulus of 200 GPa and a Poisson's ratio of 0.30. Material properties were obtained from material tests as shown in Figure 8. Engineering stress-strain parameters were entered and isotropic hardening was specified. Axial force was first applied and then held constant. After that, displacements were applied in the same way that they were in the experimental tests. The column was considered to be fixed at its base (encastre), and out-of-plane translation and twisting were also restricted at the top of the column, as they were in the experiment. Second order effects, which relate to P-delta and buckling, were turned off to evaluate column shortening without the effect of buckling in these preliminary analyses. It should be noted that P-delta effects were not significant in the experimental set-up. Here, the top and bottom of the column were fixed in position, and a moment was applied at the base (MacRae et al. 1990).

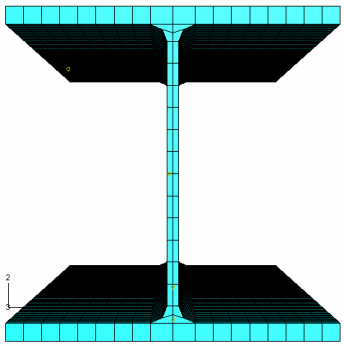

Figure 7. Column Mesh

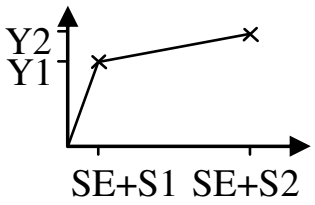

Yield Stress	Plastic Strain
294.6E6 (Y1)	0 (S1)
500E6 (Y2)	0.355 (S2)

Figure 8. Input Material Properties

The hysteretic characteristics and axial shortening from the analyses followed similar general trends to the experimental study as shown for Column C4 in Figure 9. However, in these preliminary analyses, isotropic hardening caused an artificial strength increase, and the Bauschinger effect has disappeared.

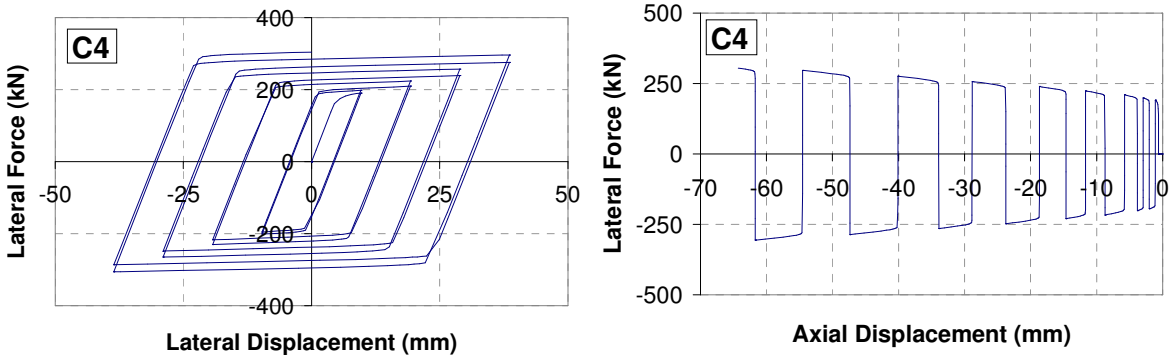

(a) (b)

Figure 9. Column C4 (N^*/N_y = 0.4) Hysteretic and Axial Deformation Curves

Column C4 axial shortening is shown against cumulative inelastic rotation in Figure 10a. The axial shortening from ABAQUS is greater than that found experimentally by MacRae (1990). A curve fit was made to the ABAQUS results (Hyde-2006) based on Equation 4 using a coefficient of 0.47 rather than 0.50 because the neutral axis is slightly in from the outer edge of the flange.

Axial shortening is shown against cumulative inelastic rotation for columns with different axial forces in Figures 10b-d. The number after the "C" is the axial force ratio multiplied by 10. For example,

column C7 has an axial force ratio of 0.70. It may be seen that the curve fit equation, Hyde 2006, agrees well with the ABAQUS results. Hyde (2006), and this study using ABAQUS, showed that for axial force ratios significantly greater than 0.22 (= A_w/A for the 250UC73 section), the neutral axis is in the flange and axial shortening is not dependent on the actual axial force. The experimental equations, from Figure 4, estimate a displacement which is about 0.4 of that from Hyde/ABAQUS for axial force ratios less than 0.22. For axial force ratios greater than 0.58, Hyde/ABAQUS and experimental results are similar. In between 0.22 and 0.58 the difference varies with the axial force. Strain hardening in the steel may be responsible for this difference. The ratio of F_u/F_y is 1.64 in tension, and will be greater in compression. Increasing N_y in Equation 4 by 2.5 times would match the experiments.

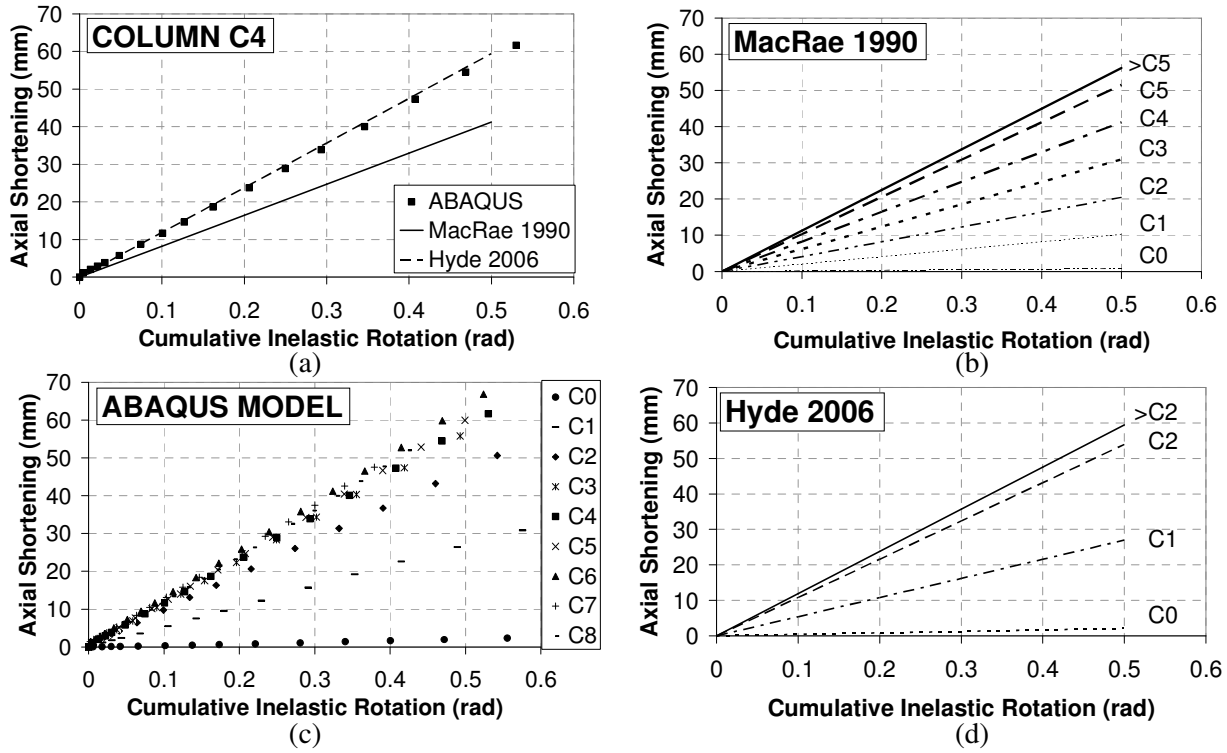

Figure 10. Column Axial Deformation Comparisons

3 MODIFICATIONS TO REDUCE AXIAL SHORTENING

Large amounts of axial shortening have been observed both experimentally and analytically in steel columns as described above. If axial shortening can be avoided, the frame is likely to perform better. One method to do this is proposed below. It involves placing extra steel at the middle of the section. The amount of steel required is related to the expected maximum axial force on the section. If the maximum axial force ratio expected is N^*/N_y, then the area of extra steel, A_{extra}, should be $(N^*/N_y).A$, where A is the total original section area. The steel added should be compact in order to avoid buckling. It should be connected with welds of sufficient capacity to ensure that the yield force in this extra steel can be developed. Figure 10 shows an original section with added steel. In the ABAQUS model, the extra steel was extended over the entire length of the member.

Placing extra steel at the centre of the section has the following advantages. For bending about the strong axis, the stiffness is hardly changed, and the moment capacity is similar to that for a bare section (i.e. M_p) for a greater range of axial forces, as shown in Figure 11. Secondly, the neutral axis is expected to remain within the region of added steel near the section centroid. This will result in almost no axial shortening. In the out-of-plane loading direction, the stiffness and strength of the column will be increased at the base, but the amount of axial shortening will be reduced. The out-of-plane direction is not as critical as the in-plane direction because the neutral axis is less likely to migrate as far from the centre of the section.

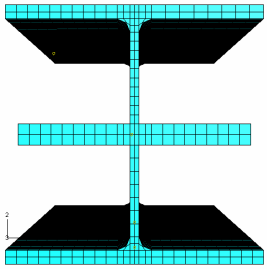

Figure 10. Modified Section

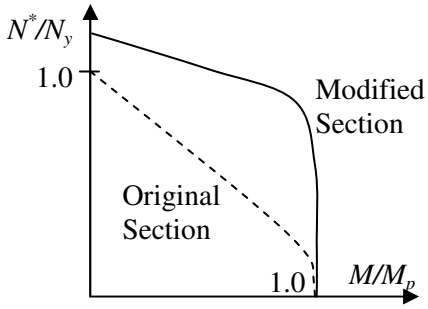

Figure 11. Idealized Moment-Axial Force Interaction Curves

The modified section is stronger than the unmodified section, as shown in Figure 12, because neutral axis for the modified section is closer to the centroid.

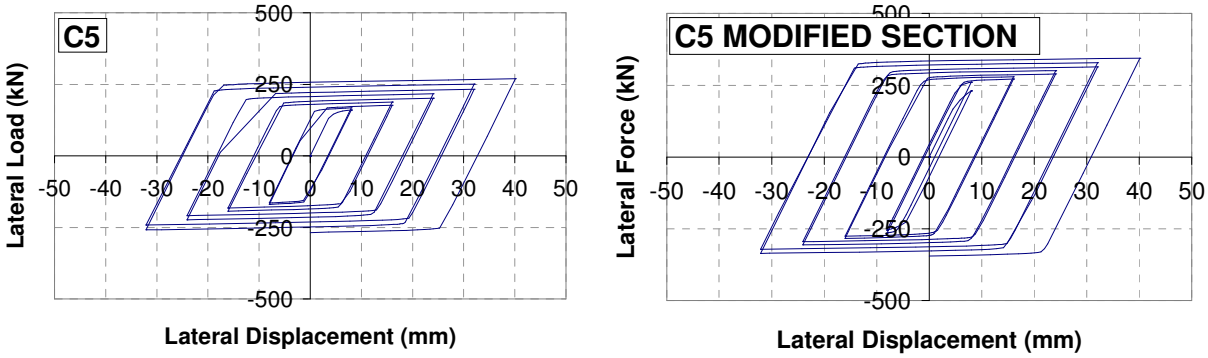

(a) Standard Section (b) Modified Section

Figure 12. Comparison of Hysteretic Curves

The axial displacement for Column C5, both with and without the modification, is shown in Figure 13. It may be seen that the modification is effective in limiting the amount of column axial shortening.

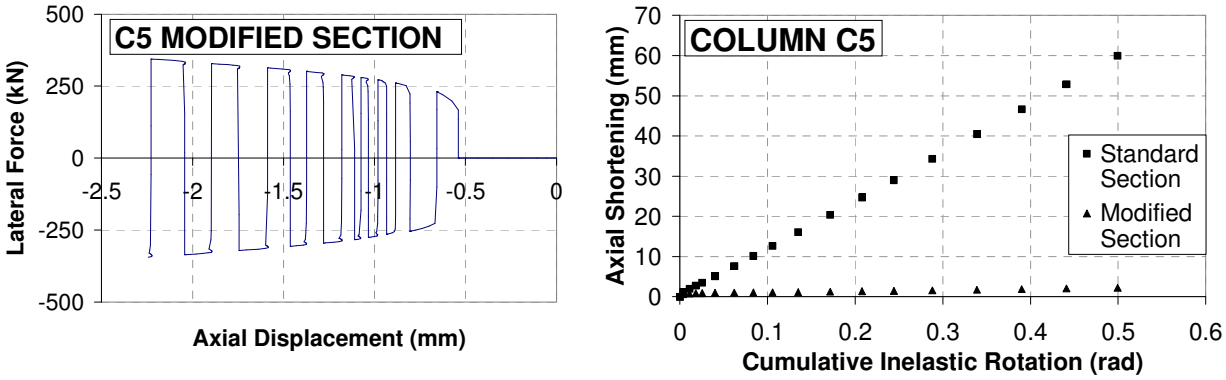

(a) (b)

Figure 13. Effect of Modification on Axial Shortening

Because the majority of column yielding is expected at the base of the structure as shown in Figure 1, modified columns are more likely to be required here than at other locations within the frame.

4 FUTURE WORK

While the preliminary analyses described in this paper provide an indication of the extent of column axial shortening and a method to mitigate its adverse effects, further finite element analyses will be carried out to improve the modelling accuracy. The C3D8I (incompatible mode) element, rather than the C3D8R element, may be better as it has enhanced bending behaviour. Alternatively, or additionally, more elements over the thickness of the flanges and web may be used to capture local buckling effects. Combined kinematic/isotropic hardening will be used in place of the present isotropic model (Mago 2003) since it is more appropriate for cyclic loading. A sensitivity study to check the effect of the mesh and the type of solid element will also be carried out.

Once the research team is happy with the results from these analyses, analyses of columns with other configurations will be performed. Simple methods for estimating axial displacements will then be developed for columns with a range of configurations, sizes and axial forces. This information will be used to calibrate a fibre hinge in the program RUAUMOKO (Carr, 2005). Dynamic inelastic time history analysis of a structure incorporating axial shortening will then be carried out to evaluate axial shortening in a realistic frame.

5 CONCLUSIONS

Equations were derived from first principles and finite element analyses were conducted to model the behaviour of compact steel I-shaped columns subject to axial force and reverse cyclic lateral displacements. It was found that:

1. The equations developed estimated column axial shortening as a function of the cumulative inelastic rotation and the axial force level. They show that for axial forces greater than a critical level, the rate of axial shortening does not increase with greater axial force. The first principles analysis provides physical understanding of the column behaviour.
2. The equations fit experimental results well for columns with high axial forces before buckling occurs. For lower axial forces, a method to correct the equations is proposed, which results in a good data fit.
3. Even though simple assumptions were used to develop the finite element model, the model provides a reasonable approximation to the hysteretic and axial shortening behaviour observed in experimental tests. It also matches the derived equations well.
4. The amount of axial shortening in the cantilever columns was sometimes more than 7% of the length. In order to prevent the possibility of very large amounts of column shortening during an earthquake, a method to mitigate the axial shortening is proposed in which extra steel is added at the centre of the section. Simple methods can be used to determine the amount of steel required. Finite element analyses showed that axial shortening is virtually eliminated.

ACKNOWLEDGMENTS:

The authors gratefully acknowledge the financial support of Steel Construction New Zealand for funding the second author, as well as the support of the University of Canterbury. Any opinions expressed in this paper are those of the authors, and they do not necessarily represent those of the sponsoring organisations.

REFERENCES:

ABAQUS 2004. ABAQUS/Standard User's Manual. ABAQUS, Inc., Providence, RI, USA.

Carr A. J. 2005. "RUAUMOKO", *User Guide, Department of Civil Engineering, University* of Canterbury, New Zealand.

Clifton G. C. 2005. "Semi-Rigid Joints for Moment-Resisting Steel Framed Seismic-Resisting Systems", Ph.D. *Thesis Report*, University of Auckland, Auckland, New Zealand.

Hyde K., MacRae G. A., Walpole W. R. and Moss P., 2006. "Column Axial Shortening Effects in Steel Frames", Department of Civil Engineering Report to Steel Construction New Zealand, University of Canterbury, New Zealand.

Feeney M.J. and Clifton G.C. 1994 with update 2000. “Seismic Design Procedures for Steel Structures”, *HERA Report* R4-76 with update, New Zealand Heavy Engineering Research Association, Manukau City, New Zealand.

MacRae G. A., Carr A. J. and Walpole W. R. 1990. "The Seismic Response of Steel Frames", *Department of Civil Engineering Research Report* 90-6, University of Canterbury, New Zealand.

Mago N. 2003. "Finite Element Analysis of Moment End Plate Connections", *HERA Report* R4-117, New Zealand Heavy Engineering Research Association, Manukau City, New Zealand.

SNZ. 1997. "NZS 3404:Part 1:1997 Steel Structures Standard", *Standards New Zealand*, Wellington, New Zealand.